

Multi-StyleGS: Stylizing Gaussian Splatting with Multiple Styles

Yangkai Lin¹, Jiabao Lei², Kui jia^{2*}

¹South China University of Technology

²School of Data Science, The Chinese University of Hong Kong, Shenzhen
202210182091@mail.scut.edu.cn, jiabaolei@link.cuhk.edu.cn, kuijia@cuhk.edu.cn



Figure 1: With a set of multi-view images of a 3D scene and several specified style images, our method can transfer artistic styles to the 3D scene, creating high-quality stylized images of novel views with consistency.

Abstract

In recent years, there has been a growing demand to stylize a given 3D scene to align with the artistic style of reference images for creative purposes. While 3D Gaussian Splatting (GS) has emerged as a promising and efficient method for realistic 3D scene modeling, there remains a challenge in adapting it to stylize 3D GS to match with multiple styles through automatic local style transfer or manual designation, while maintaining memory efficiency for stylization training. In this paper, we introduce a novel 3D GS stylization solution termed Multi-StyleGS to tackle these challenges. In particular, we employ a bipartite matching mechanism to automatically identify correspondences between the style images and the local regions of the rendered images. To facilitate local style transfer, we introduce a novel semantic style loss function that employs a segmentation network to apply distinct styles to various objects of the scene and propose a local-global feature matching to enhance the multi-view consistency. Furthermore, this technique can achieve memory-efficient training, more texture details and better color match. To better assign a robust semantic label to each Gaussian, we propose several techniques to regularize the segmentation network. As demonstrated by our comprehensive experiments, our approach outperforms existing ones in produc-

ing plausible stylization results and offering flexible editing.
code: <https://github.com/SCUTykLin/Multi-StyleGS.git>

Introduction

Artistic creation has attracted considerable attention, with aesthetic 3D content creation being one of the urgent demands in recent years. Stylizing an already acquired 3D scene is the primary approach to obtain artistic 3D content. In this paper, our focus is on the task of 3D scene stylization, where we aim to transfer reference styles specified by multiple style images to the 3D scene.

Previous work on 3D stylization (Huang et al. 2022; Wang et al. 2023; Pang, Hua, and Yeung 2023; Jung et al. 2024) has predominantly utilized the Neural Radiance Field (NeRF) as a scene representation (Mildenhall et al. 2020). While NeRF is compact and capable of achieving photo-realistic rendering results, it is limited to implicit editing and faces significant performance challenges due to the utilization of a heavy and high-dimensional Multi-Layer Perceptron (MLP) network for scene representation. Balancing computational time and result quality requires a delicate trade-off. Despite some advancements (Müller et al. 2022; Reiser et al. 2021; Sun, Sun, and Chen 2022; Fridovich-Keil et al. 2022; Chen et al. 2022; Hu et al. 2023; Barron et al. 2023) aimed at mitigating the performance issues of NeRF

*Corresponding author.

in practical applications, these challenges still persist. Recently, a significant portion of the work on 3D stylization has concentrated on global stylization (Zhang et al. 2022; Nguyen-Phuoc, Liu, and Xiao 2022; Liu et al. 2023; Chiang et al. 2022a), where the same style pattern is applied uniformly to all parts of the 3D content. However, this approach can be suboptimal as not all regions should be treated equally, limiting flexibility and editability. Another portion of the work focus on the local stylization (Miao et al. 2024; Zhang et al. 2023). However, they can only stylize simple scenes (Mildenhall et al. 2019) and struggle to ensure multi-view consistency. Furthermore, techniques that employ Gaussian Splatting (GS) (Kerbl et al. 2023) frequently encounter memory bottleneck issues, impeding the progress for further applications.

To address these challenges, we introduce a novel 3D stylization solution called Multi-StyleGS. This method is designed to deliver flexible and efficient image-based stylization of 3D scenes by empowering explicit local editing.

Specifically, we choose GS (Kerbl et al. 2023) as our base representation, for its real-time rendering performance and explicit characteristic. While promising, we have noted a substantial increase in memory usage and the emergence of multi-view inconsistency in feature matching. To address these challenges, we introduce a novel semantic style loss to mitigate the problem of excessive memory consumption and multi-view inconsistency. Furthermore, to enable local stylization on semantic regions, we introduce an additional semantic feature for each GS, and update them during optimization. This enhancement facilitates automatic local style transfer for region correspondences between multiple style images and the 3D scene.

Technically, we perform local style transfer as an additional post-processing step after capturing the original geometry and appearance of the 3D scenes using GS. During the stylization process, we solely optimize the appearance of Gaussians. In addition to reconstruct 3D scene, we introduce an extra segmentation attribute that divides the Gaussians of the scene into multiple parts and paired with multiple style images through an effective bipartite matching mechanism (Luan et al. 2017) to automatically establish local region correspondences based on their feature similarity or manual designation. Subsequently, a novel multi-style loss is applied to guarantee local editability. Additionally, we observed a multi-view inconsistency issue. Inspired by (El Bani et al. 2024), we utilize DINOv2 (Oquab et al. 2023) to extract global features and introduce local-global matching for enhanced multi-view consistency with our novel multi-style loss, improving consistency, texture details, and color accuracy. To address the potential issue of segmentation error due to the high degree of freedom of Gaussians, we introduce Gaussian smoothing regularization to alleviate this problem. Additionally, in order to mitigate the semantic ambiguity problem, we develop a technique called semantic importance filtering, which leverages semantic labels to effectively eliminate those Gaussians exhibiting semantic uncertainty; a negative entropy regularization term is also applied to each Gaussian to enforce semantic clarity. Our segmentation approach leverages SAM’s (Kirillov et al. 2023) capa-

bility, which we apply to the 3D scene to enhance multi-view consistency.

Our solution is able to handle styles from one single image or multiple images. Extensive experiments conducted on various datasets (Knapitsch et al. 2017; Mildenhall et al. 2019) substantiate the efficacy of our method in generating high-quality, locally matched stylized images in real-time. To summarize, our main contributions are:

- A novel GS-based approach for local stylization of 3D scenes, facilitating the transfer of multiple artistic styles from one or several 2D images to 3D scenes.
- A new style loss that adopts bipartite matching assignment between multiple style image regions and GS points to enable (automatic) local style transfer.
- A local-global feature matching solution to improve multi-view consistency.
- Several regularization terms for removing noisy Gaussians and accuracy segmentation.

Related Works

Overview of 3D Style Transfer

Conventional approaches to stylize 3D scenes use explicit representations like point clouds (Huang et al. 2021; Mu et al. 2022) or meshes (Mu et al. 2022; Michel et al. 2022; Kato, Ushiku, and Harada 2018; Höllein, Johnson, and Nießner 2022). These approaches, however, is error-prone and may fail to capture geometry and texture details. NeRF (Mildenhall et al. 2020) encodes a 3D scene using a neural network, making it a more suitable representation for downstream stylization tasks compared to explicit ones. A common approach to stylizing a NeRF is to optimize and constrain its rendered images to a specific style using content loss and style loss. snerf, arf and ins (Nguyen-Phuoc, Liu, and Xiao 2022; Zhang et al. 2022; Fan et al. 2022) follow this line and optimizes neural networks using style loss. snerf renders blurry results due to refine geometry without supervision, and arf fixes the geometry branch and proposes nearest-neighbor feature matching loss to capture details. ins decouples NeRF to allow for separately encoding of representations.

Their results do not support diverse stylization results and typically stylize only the foreground of the scenes. HyperNet (Chiang et al. 2022b) uses a hypernetwork to predict the weights of MLP to speed up stylization. LsNeRF (Pang, Hua, and Yeung 2023) introduces a region-matching style loss designed to enhance local stylization of the 3D scenes. Yet, this method faces limitations as it cannot concurrently assimilate styles from multiple images into a single 3D scene. Moreover, it is unable to maintain multi-view stylistic consistency. Our work introduces a matching mechanism (Pang, Hua, and Yeung 2023) to establish region correspondences and a novel style loss to support local style transfer. Besides, thanks to the use of explicit representation of GS (Kerbl et al. 2023), we can nicely stylize the background as well.

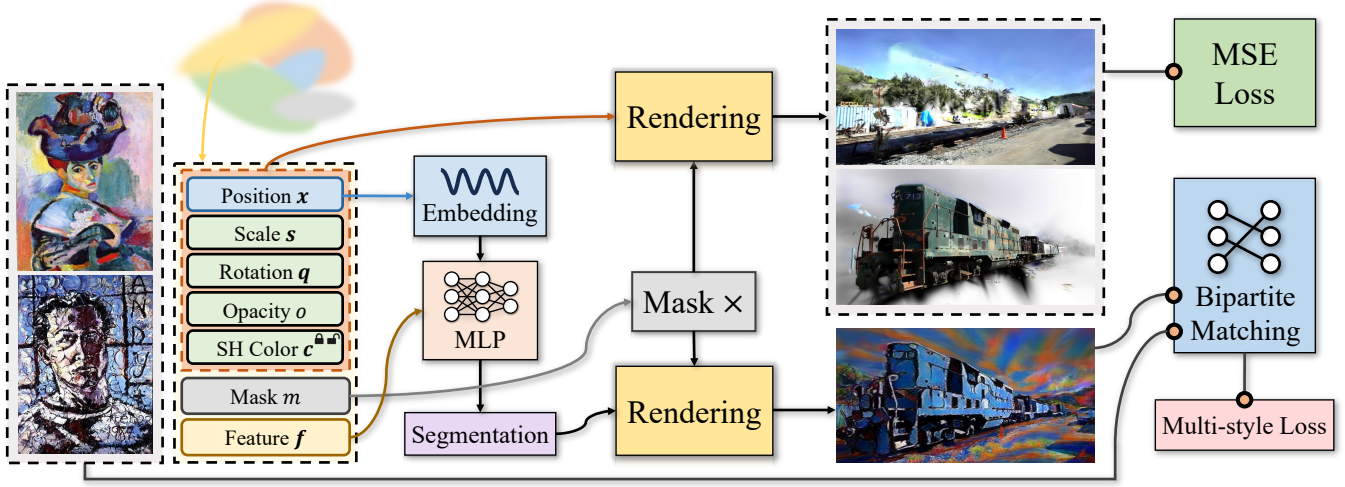


Figure 2: Overview of our pipeline. It firstly reconstructs a GS model from multiple training images, and then stylize the scene using bipartite matching with multiple styles. Upon completion, it can produce consistent free-viewpoint stylized renderings.

Memory-efficient 3D Style Transfer

However, such methods are very memory-inefficient in practice. ARF (Zhang et al. 2022) propose a deferred back-propagation method to enable optimization of memory-intensive NeRF. StyleRF (Liu et al. 2023) proposes a deferred style transformation of 2D feature maps to greatly reduces memory footprint. These approaches are all developed based on NeRF (Mildenhall et al. 2020) and are not applicable to GS (Kerbl et al. 2023). Our novel semantic style loss can achieve memory-efficient training, which enables efficient training on a single RTX 3090.

3D Local Stylization

Another line of work (Pang, Hua, and Yeung 2023; Zhang et al. 2023; Miao et al. 2024) investigates local stylization methods, which allow for diverse styles on local regions. However, most of the work can only stylize relatively simple scenes and cannot ensure multi-view consistency. Our method proposes a local-global matching to tackle this issue and conducts extensive experiments on various datasets (Mildenhall et al. 2019; Knapitsch et al. 2017).

Preliminary of Gaussian Splatting

Gaussian Splatting (GS) (Kerbl et al. 2023) represents a 3D scene with a set of 3D Gaussians. Each Gaussian consists of a center location $\mu \in \mathbb{R}^3$, a covariance matrix $\Sigma \in \mathbb{R}^{3 \times 3}$. The covariance matrix Σ can be decomposed into a rotation matrix $R \in \mathbb{R}^{3 \times 3}$ and a diagonal scaling matrix $S \in \mathbb{R}^{3 \times 3}$ as shown by

$$\Sigma = RSS^T R^T. \quad (1)$$

To render novel views, splatting is utilized to project 3D Gaussians onto 2D canvas. This technique involves a viewing transformation denoted by $W \in \mathbb{R}^{3 \times 3}$ and Jacobian $J \in \mathbb{R}^{2 \times 3}$ of the affine approximation of the projective transformation. The 2D covariance matrix $\hat{\Sigma} \in \mathbb{R}^{2 \times 2}$ can then be given as

$$\hat{\Sigma} = JW\Sigma W^T J^T. \quad (2)$$

We finally leverage α -blending of N overlapped Gaussians at a pixel to accumulate color by

$$c = \sum_{i=1}^N c_i \alpha_i \prod_{j=1}^{i-1} (1 - \alpha_j), \quad (3)$$

where $c \in \mathbb{R}^3$ is the rendered pixel color, $c_i \in \mathbb{R}^3$ and $\alpha_i \in \mathbb{R}$ are color and density of the i -th Gaussian point, respectively.

Our Method

Multi-StyleGS consists of two stages: the reconstruction stage, where a base GS model is trained to recover the original scene and additionally learn semantic correspondences, and the stylization stage, where the GS model is further refined to adjust its appearance to multiple styles specified by the correspondences.

Gaussian Splatting with Semantic Features

To establish local region correspondences for local style transfer, we leverage segmentation maps and match local regions in 3D scenes with those in style images. In particular, we enhance GS by incorporating an extra segmentation branch, as illustrated in Figure 2. In addition to the existing attributes of the Gaussians (e.g., color and opacity), we introduce a new trainable feature e_i for each Gaussian (Ye et al. 2023; Zhou et al. 2024). This feature e_i is subsequently decoded by a tiny MLP to predict a semantic category.

To optimize the feature e_i and the tiny MLP, we render these semantic features into 2D images in a differentiable manner. Specifically, we have the following formula for feature integration:

$$e = \sum_{i=1}^N e_i \alpha_i \prod_{j=1}^{i-1} (1 - \alpha_j), \quad (4)$$

where $e \in E$ is the rendered feature and E denotes the rendered feature map. The feature e subsequently passes

through a softmax function to calculate the cross-entropy loss \mathcal{L}^{seg} . However, to compute \mathcal{L}^{seg} , we need ground-truth semantic labels. We use SAM (Kirillov et al. 2023) to automatically generate semantic labels for each 2D image and employ a well-trained zero-shot tracker (Cheng et al. 2023) to propagate and associate semantic labels (Ye et al. 2023). Back-propagation is employed to optimize the feature \mathbf{e}_i and parameters of the tiny MLP.

However, we observe that updating each Gaussian point individually can lead to noisy and unstable outcomes due to the stochastic optimization nature and the restricted granularity of points. To address the issues, we leverage a locality assumption: neighboring points should exhibit similar characteristics. We introduce a regularization loss to enhance the smoothness of segmentation results based on k -nearest neighbor (KNN) by

$$\mathcal{L}^{\text{KNN}} = \sum_i \sum_{j \in \mathcal{N}_i} \|\mathbf{e}_i - \mathbf{e}_j\|_2^2 e^{-\frac{\|\mu_i - \mu_j\|}{\sigma}}, \quad (5)$$

where \mathcal{N}_i gathers k nearest neighbors for the i -th Gaussian, and $\sigma \in \mathbb{R}_{>0}$ determines the influence radius. The essence of \mathcal{L}^{KNN} lies in weighting the similarity differences according to the influence of their distances. Our assumption encourages local smoothness, avoids excessive randomness, and increases the granularity of influence.

Moreover, we notice that one Gaussian point may be responsible for multiple objects, leading to semantic ambiguity which is unwanted. We incorporate a negative entropy regularization term:

$$\mathcal{L}_{\text{NE}} = - \sum_{i=1}^N \text{softmax}(\mathbf{e}_i) \log(\text{softmax}(\mathbf{e}_i)), \quad (6)$$

to enforce each point to choose only one category, eliminating such an ambiguity.

However, some points may be of less semantic importance. We utilize a semantic importance filter to eliminate those with less semantic significance. Specifically, we additionally assign a learnable mask attribute $m \in \mathbb{R}$ to individual Gaussian (Lee et al. 2023) to assess its importance, and utilize semantic labels \mathbf{e}_i to select Gaussians without semantic ambiguity. We also employ the straight-through estimator (Bengio, Léonard, and Courville 2013) for gradient propagation. We apply a mask $m^b \in \{0, 1\}$ to the scale vector $\mathbf{s} \in \mathbb{R}^3$ (diagonal elements of \mathbf{S}) and the opacity $o \in \mathbb{R}$ by $\hat{\mathbf{s}} = m^b \mathbf{s}$ and $\hat{o} = m^b o$, respectively, where the binary mask m^b can be obtained by

$$m^b = \text{sg} [v^b - \sigma(m)] + \sigma(m), \quad (7)$$

$$\text{with } v^b = \mathbb{1}_{\sigma(m) > \epsilon_0} \vee \mathbb{1}_{\max(\text{softmax}(\mathbf{e}_i)) > \epsilon_1},$$

where $\epsilon_0 \in \mathbb{R}$ and $\epsilon_1 \in \mathbb{R}$ are thresholds, “sg” is to stop gradients, σ is the sigmoid function, $\mathbb{1}_A$ is an indicator of event A , and \vee is logical OR operator. During reconstruction, the GS model optimizes the scale, opacity, and mask attributes simultaneously. This approach enables a more holistic consideration of both scale and opacity when assessing the importance of Gaussian components. To promote the decima-

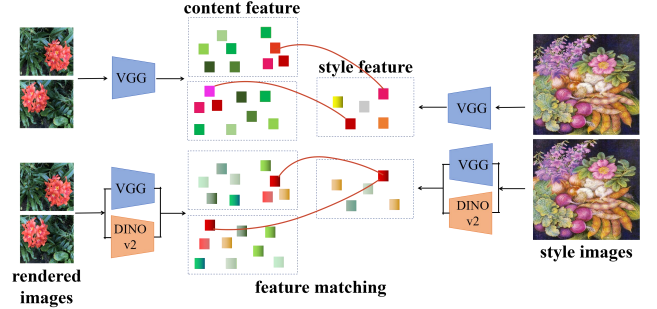


Figure 3: The VGG features do not ensure consistency across different viewpoints, leading to the same object being associated with distinct features when viewed from various angles. However, by incorporating DINOv2, we can maintain local details while also achieving enhanced consistency in feature matching, regardless of the viewing perspective.

tion of redundant Gaussians, we introduce a mask regularization term given by

$$\mathcal{L}^{\text{mask}} = \sum_m \sigma(m). \quad (8)$$

We note that by incorporating $\mathcal{L}^{\text{mask}}$, our model facilitates the automatic elimination of Gaussians through gradient control. By adjusting the weighting coefficient of $\mathcal{L}^{\text{mask}}$, we can achieve a more optimal balance between rendering quality and memory footprint. At specific iterations, we remove certain unnecessary Gaussians based on m^b .

Preliminary of Style Loss

Given a pair of rendered output image I and style image S , the style loss typically operates on high-level features $\mathbf{f}_I = F(I)$, $\mathbf{f}_S = F(S)$, where F is a pretrained VGG19 (Simonyan and Zisserman 2015a) network. For instance, StyleGaussian (Liu et al. 2024) employs AdaIN for stylistic transformation, while ARF (Zhang et al. 2022) introduces a nearest-neighbor feature matching (NNFM) loss to achieve style transfer. The NNFM loss introduced in (Zhang et al. 2022) uses the following formulation,

$$\mathcal{L}_{\text{NNFM}}^{\text{naive}} = \sum_{f_i \in \mathbf{f}_I} \min_{f_j \in \mathbf{f}_S} d(f_i, f_j), \quad (9)$$

where every individual feature vector $f_i \in \mathbf{f}_I$ is paired with the closest style feature $f_j \in \mathbf{f}_S$ according to cosine distance d . However, the style loss is to match the global statistics between the rendered output image I and style image S , and can not support diverse stylization results. We incorporate bipartite matching to augment NNFM loss to support local style transfer, which will be detailed in the next coming section.

However, VGG feature is 2D local and has no 3D awareness. Using VGG features only for matching can lead to multi-view inconsistency issues. Moreover, a substantial increase in memory usage is observed when utilizing GS as the base representation for stylization. To address these issues, we propose a novel semantic style loss.

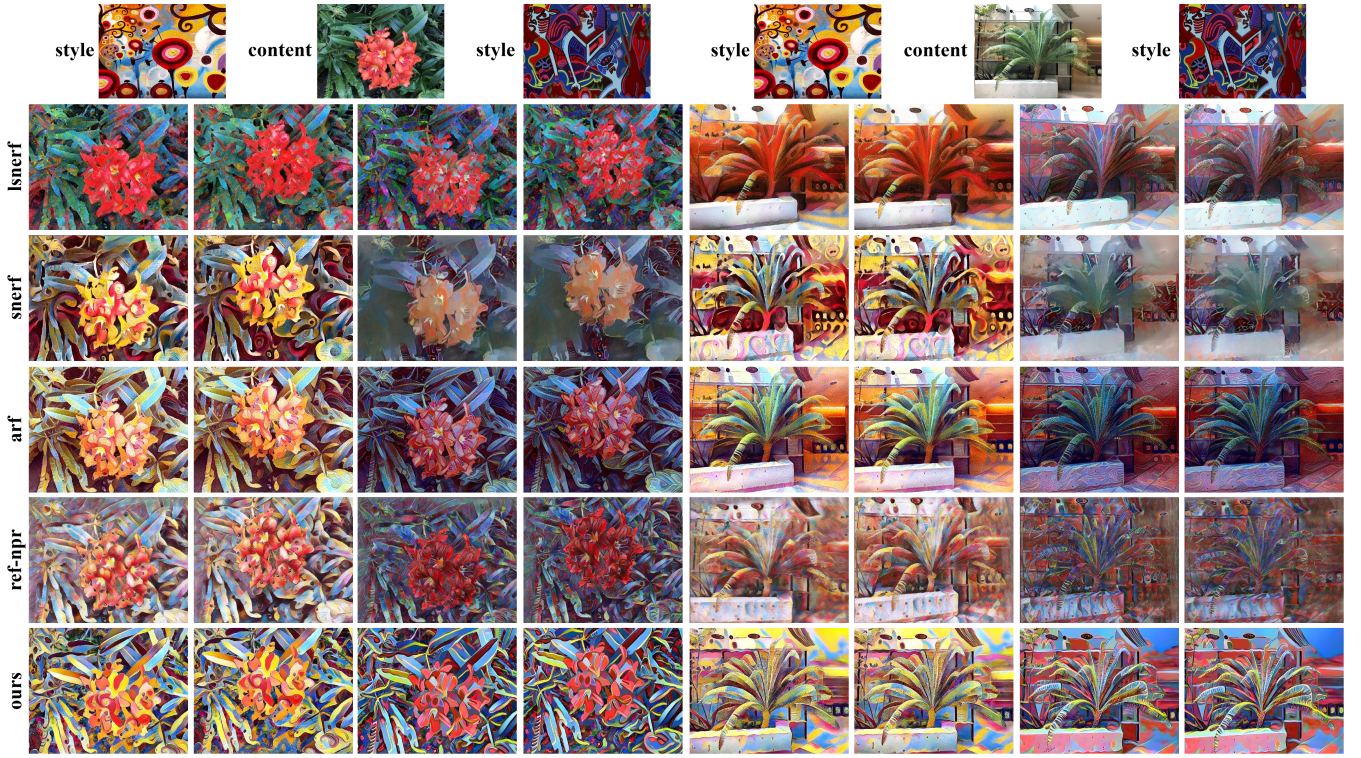


Figure 4: Qualitative comparisons with snerf (Nguyen et al. 2022), arf (Zhang et al. 2022), ref-npr (Zhang et al. 2023) and lsnerf (Pang, Hua, and Yeung 2023) on *flower* and *fern* scenes (Mildenhall et al. 2019).

Semantic Multi-style Loss

To facilitate local style transfer, we firstly establish region correspondences for the Gaussian point set $\{g_i\}_{i=1}^N$ of the scene and the set of input style images $\{S_i\}_{i=1}^M$. After reconstruction, the feature e_i of each Gaussian will indicate the semantic label to which the object it belongs, categorizing the Gaussians into C distinct classes. The initial step in our pipeline involves partitioning $\{g_i\}_{i=1}^N$ into multiple point set $\{G_i\}_{i=1}^C$ as show in Figure 2.

Local-global Feature Matching Since Gaussian points, when observed from various perspectives, may align with distinct style features, resulting in multi-view inconsistency, as illustrated in Figure 3. We found that features from VGG tend to suffer from such a problem stemming from poor global consistency.

One paper (El Banani et al. 2024) assessed the 3D awareness of visual models and posits that DINOv2 (Oquab et al. 2023) demonstrates superior 3D consistency. Therefore, we extract DINOv2 feature and VGG feature and concatenate them along the channel dimension, then perform nearest feature matching on concatenative feature as follows,

$$\mathbf{C}_S = \text{concat}(\mathbf{f}_S, \phi(S)), \mathbf{C}_I = \text{concat}(\mathbf{f}_I, \phi(I)), \quad (10)$$

$$\mathcal{L}_{\text{NNFM}} = \sum_{f_i \in \mathbf{C}_I} \min_{f_j \in \mathbf{C}_S} d(f_i, f_j), \quad (11)$$

where ϕ is the DINOv2 feature extractor, “concat” is to concatenate two feature maps along the channel dimension. VGG feature can provide local details and DINOv2 feature

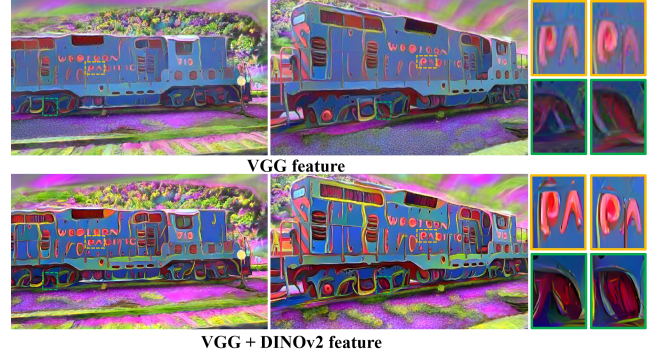


Figure 5: Comparing the stylized results, from various perspectives, the same object may correspond to different VGG features, averaging out the details (as seen in subfigures with orange borders) or displaying varying colors (as seen in subfigures with green borders). DINOv2 enhances the global consistency that VGG features lack, ensuring consistent guidance across different viewpoints.

can provide global consistency. $\mathcal{L}_{\text{NNFM}}$ not only enhances multi-view consistency but also better improves matching results, ensuring that the same area, when viewed from another perspective, exhibits consistency and is endowed with richer and clearer details, as shown in Figure 5.

Local Style Loss To prevent multiple scene regions from being stylized with the same local pattern, we incorporate a bipartite matching mechanism (Pang, Hua, and Yeung 2023) to automatically identify local region correspondences be-

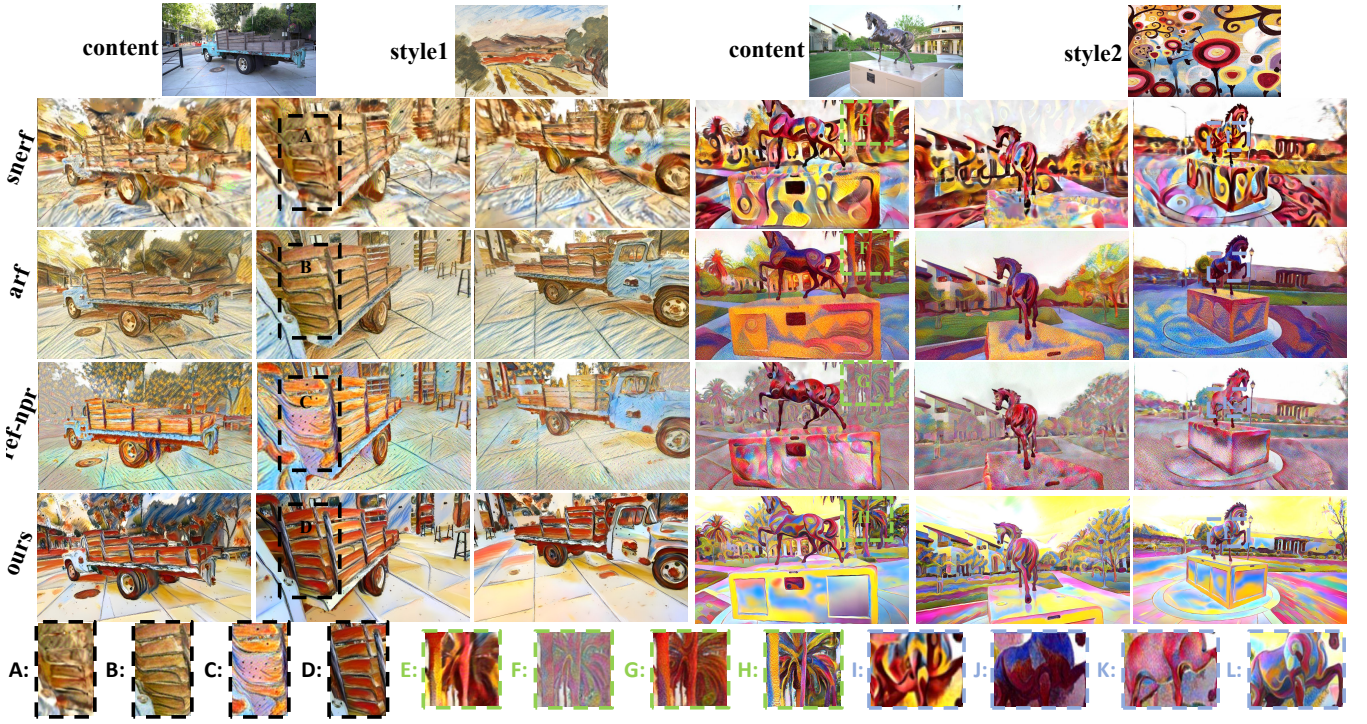


Figure 6: Qualitative comparisons with snrf(Nguyen et al. 2022), arf(Zhang et al. 2022) and ref-npr(Zhang et al. 2023) on tnt datasets in single style setting. **Black boxes (A-D): inconsistency may lead to blurry results; green boxes (E-H): previous solutions may produce incomplete stylized results; blue boxes (I-L): our method can preserve texture details.** Our solution is effective in addressing all of these problems.

tween multiple point set $\{G_i\}_{i=1}^C$ and multiple style images $\{S_i\}_{i=1}^M$. We construct a cost matrix $\mathbf{Q} \in \mathbb{R}^{C \times M}$, where each entry Q_{ij} represents the correlation between regions G_i and S_j . We first render each point set G_i into image I_i , then utilize VGG19 (Simonyan and Zisserman 2015b) to extract features from both the rendered image I_i and the stylized image S_j . The correlation is determined by the cosine feature distance between the means of features of I_i and S_j .

Given the cost matrix \mathbf{Q} , an optimal mapping $\mathcal{M} : [1, C] \mapsto [1, M]$ can be generated by Hungarian algorithm. Our multi-style loss can be finally formulated as

$$\mathcal{L}^{\text{style}} = \sum_{j=1}^C \sum_{\mathbf{f} \in C_{I_j}} \min_{\substack{k=\mathcal{M}(j) \\ \mathbf{g} \in C_{S_k}}} d(\mathbf{f}, \mathbf{g}), \quad (12)$$

where \mathbf{f} and \mathbf{g} are pixel-wise features, d measures the cosine distance. Through the minimization of our multi-style loss, we augment the GS model with the ability to perform stylization with multiple styles. Such a design not only enables local style transfer but also significantly alleviates the burden on GPU memory. By strategically categorizing Gaussians into several distinct categories, our model circumvents the need to apply splatting to all Gaussians in a single pass. Moreover, the stylization process with these categorized Gaussians naturally ensures that the resulting appearance exhibits seamless continuity and unambiguity.

Training Details

Reconstruction stage. Our GS model is trained with

$$\mathcal{L}^{\text{recon}} + \lambda^{\text{seg}} \mathcal{L}^{\text{seg}} + \lambda^{\text{KNN}} \mathcal{L}^{\text{KNN}} + \lambda^{\text{NE}} \mathcal{L}^{\text{NE}} + \lambda^{\text{mask}} \mathcal{L}^{\text{mask}}, \quad (13)$$

where $\mathcal{L}^{\text{recon}}$ is the Mean Squared Error (MSE) reconstruction loss as outlined in (Kerbl et al. 2023). We typically assign values of $\lambda^{\text{seg}} = 0.02$, $\lambda^{\text{KNN}} = 0.005$, $\lambda^{\text{NE}} = 0.005$.

Stylization stage. After reconstruction, we can obtain a region mapping \mathcal{M} . During the stylization stage, we utilize the mapping \mathcal{M} and train the model by minimizing

$$\lambda^{\text{cont}} \mathcal{L}^{\text{cont}} + \lambda^{\text{style}} \mathcal{L}^{\text{style}}, \quad (14)$$

where $\mathcal{L}^{\text{cont}}$ is the content loss, which measures the MSE between the encoded feature map and the ground truth.

Experiments

Datasets

We conducted extensive experiments on a diverse set of real-world scenes, including outdoor environments from the Tanks and Temples (shortened as “tnt” in our paper) dataset (Knapitsch et al. 2017) and forward-facing scenes from the liff dataset (Mildenhall et al. 2019).

Evaluation Metrics

We use Single Image Frechet Inception Distance (SIFID) (Ding et al. 2022) to evaluate the stylization similarity. We perform quantitative comparisons on multi-view consistency (Chiang et al. 2022a). Additionally, we provide visual comparisons and results.



Figure 7: Qualitative comparisons with snarf (Nguyen et al. 2022), arf (Zhang et al. 2022) and ref-npr (Zhang et al. 2023) on tnt datasets in multiple style setting. **Yellow boxes (O, P, U, V): inconsistency can lead to blurry results; orange boxes (Q, R): incorrect color blending between multiple regions; blue boxes (S, T): our method can produce finer texture details.**

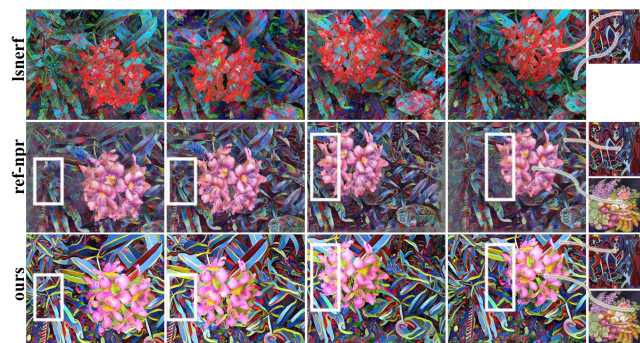


Figure 8: Qualitative comparisons with ref-npr (Zhang et al. 2023), Isnerf (Pang, Hua, and Yeung 2023). The results enclosed in the white boxes are blurred due to the multi-view inconsistency in the ref-npr. In contrast, our model has effectively ensured consistency.

Baselines

On lfff datasets (Mildenhall et al. 2019), we compare our method to the SOTA methods, *e.g.*, arf (Zhang et al. 2022), lsnerf (Pang, Hua, and Yeung 2023), snerf (Nguyen-Phuoc, Liu, and Xiao 2022) and ref-npr (Zhang et al. 2023). Arf and snerf stylize the whole scene with a style image; lsnerf establishes region correspondences between the style image and the content to support local style transfer; ref-npr stylizes scenes with a reference image and VGG matching.

Qualitative and Quantitative Comparisons

In Figure. 4, we qualitatively compare with other methods on **lfff dataset in single style setting**. Our method provides clearer colors and more accurately stylized texture. Lsnerf fails to fully transfer styles; snerf generates error geometry and produce blurred images; arf employs nnfm in VGG matching, yet suffers from incorrect color blending due to VGG’s inability of 3D awareness; ref-npr transfers styles from reference view using VGG but is limited to simple style and struggles with high-frequency signals (*fern* scene). In Figure. 8, we compare our result with two multi-style methods on **lfff datasets in multiply style setting**. Lsnerf and ref-

Methods	truck	horse	flower	Avg.
snarf (Nguyen et al. 2022)	3.00	2.7	0.78	2.16
arf (Zhang et al. 2022)	2.23	1.50	0.16	1.29
ref-npr (Zhang et al. 2023)	3.12	1.78	0.88	1.92
ours (vgg)	1.71	1.70	0.14	1.18
ours	1.55	1.21	0.14	0.96

Table 1: Quantitative comparisons of multi-view consistency. Lower scores indicate better consistency.

npr suffer from multi-view inconsistency, which results in a blurred background. Our method delivers consistent outcomes, detailed textures, and improved color matching.

In Figure. 6, we compare our results with four SOTA methods on **tnt datasets in single style setting**. Snerf generates blurry images due to geometry error; ARF underperforms in the *horse* scene due to its inability to capture fine details and maintain color consistency; ref-npr can only transfer smooth style image and render blurry background in *style2*. Our method adeptly reconstructs scenes, meticulously maintaining the original’s geometric and semantic information. Figure. 7 presents results with **multiple styles on tnt datasets**; for the *truck* scene, ref-npr struggles with backgrounds and blends with two styles, whereas our model cleanly distinguishes and separates them from the truck.

In Table. 3, we use the metrics from (Chiang et al. 2022a) to measure the consistency. We generate rendered videos for each scene and randomly sample 50 frames 5 times to calculate their consistency. Our method achieves the best multi-view consistency scores in all metrics.

Ablation Studies

Due to limited space, we move additional experimental analysis and results to the supplementary material.

Semantic Multi-style loss Semantic multi-style loss can achieve multi-style transfer and efficient training. Table. 4 shows the average number of points per iteration when using the multi-style loss to reduce GPU memory usage, *e.g.*, the truck scene that has 1M points in total, is optimized on its

style loss	truck	horse	train
multi-style loss	362,548.6	301,322.7	378,561.5
nnfm loss	1,087,646	834,546	756,747

Table 2: Ablation Study of GPU memory. Multi-style loss optimizes fewer points each time, using less GPU memory.

categorized subsets typically with 398K points for “truck” and 123K points for “ground”.

VGG feature and DINOv2 feature Figure. 5 and Table. 3 present the ablation study results of multi-view consistency. By incorporating DINOv2 features, we can achieve better outcomes with multi-view consistency.

Limitations and Future Works

We also notice that our model is incapable of instant style transfer and thus requires retraining for different styles. We will leave this for future improvement.

References

Barron, J. T.; Mildenhall, B.; Verbin, D.; Srinivasan, P. P.; and Hedman, P. 2023. Zip-NeRF: Anti-aliased grid-based neural radiance fields. *arXiv preprint arXiv:2304.06706*.

Bengio, Y.; Léonard, N.; and Courville, A. 2013. Estimating or propagating gradients through stochastic neurons for conditional computation. *arXiv preprint arXiv:1308.3432*.

Chen, A.; Xu, Z.; Geiger, A.; Yu, J.; and Su, H. 2022. Tensorf: Tensorial radiance fields. In *European Conference on Computer Vision*, 333–350. Springer.

Cheng, H. K.; Oh, S. W.; Price, B.; Schwing, A.; and Lee, J.-Y. 2023. Tracking anything with decoupled video segmentation. In *Proceedings of the IEEE/CVF International Conference on Computer Vision*, 1316–1326.

Chiang, P.-Z.; Tsai, M.-S.; Tseng, H.-Y.; Lai, W.-S.; and Chiu, W.-C. 2022a. Stylizing 3D Scene via Implicit Representation and HyperNetwork. In *Proceedings of the IEEE/CVF Winter Conference on Applications of Computer Vision (WACV)*.

Chiang, P.-Z.; Tsai, M.-S.; Tseng, H.-Y.; Lai, W.-S.; and Chiu, W.-C. 2022b. Stylizing 3D Scene via Implicit Representation and HyperNetwork. In *Proceedings of the IEEE/CVF Winter Conference on Applications of Computer Vision (WACV)*.

Ding, X.; Wang, Y.; Xu, Z.; Welch, W. J.; and Wang, Z. J. 2022. Continuous conditional generative adversarial networks: Novel empirical losses and label input mechanisms. *IEEE Transactions on Pattern Analysis and Machine Intelligence*, 45(7): 8143–8158.

El Banani, M.; Raj, A.; Maninis, K.-K.; Kar, A.; Li, Y.; Rubinstein, M.; Sun, D.; Guibas, L.; Johnson, J.; and Jampani, V. 2024. Probing the 3D Awareness of Visual Foundation Models. In *CVPR*.

Fan, Z.; Jiang, Y.; Wang, P.; Gong, X.; Xu, D.; and Wang, Z. 2022. Unified implicit neural stylization. In *European Conference on Computer Vision*, 636–654. Springer.

Fridovich-Keil, S.; Yu, A.; Tancik, M.; Chen, Q.; Recht, B.; and Kanazawa, A. 2022. Plenoxels: Radiance fields without neural networks. In *Proceedings of the IEEE/CVF Conference on Computer Vision and Pattern Recognition*, 5501–5510.

Höllein, L.; Johnson, J.; and Nießner, M. 2022. Stylemesh: Style transfer for indoor 3d scene reconstructions. In *Proceedings of the IEEE/CVF Conference on Computer Vision and Pattern Recognition*, 6198–6208.

Hu, W.; Wang, Y.; Ma, L.; Yang, B.; Gao, L.; Liu, X.; and Ma, Y. 2023. Tri-MipRF: Tri-Mip Representation for Efficient Anti-Aliasing Neural Radiance Fields. In *ICCV*.

Huang, H.-P.; Tseng, H.-Y.; Saini, S.; Singh, M.; and Yang, M.-H. 2021. Learning to stylize novel views. In *Proceedings of the IEEE/CVF International Conference on Computer Vision*, 13869–13878.

Huang, Y.-H.; He, Y.; Yuan, Y.-J.; Lai, Y.-K.; and Gao, L. 2022. Stylizednerf: consistent 3d scene stylization as stylized nerf via 2d-3d mutual learning. In *Proceedings of the IEEE/CVF Conference on Computer Vision and Pattern Recognition*, 18342–18352.

Jung, H.; Nam, S.; Sarafianos, N.; Yoo, S.; Sorkine-Hornung, A.; and Ranjan, R. 2024. Geometry Transfer for Stylizing Radiance Fields. In *Proceedings of the IEEE/CVF Conference on Computer Vision and Pattern Recognition*, 8565–8575.

Kato, H.; Ushiku, Y.; and Harada, T. 2018. Neural 3d mesh renderer. In *Proceedings of the IEEE conference on computer vision and pattern recognition*, 3907–3916.

Kerbl, B.; Kopanas, G.; Leimkühler, T.; and Drettakis, G. 2023. 3D Gaussian Splatting for Real-Time Radiance Field Rendering. *ACM Transactions on Graphics*, 42(4).

Kirillov, A.; Mintun, E.; Ravi, N.; Mao, H.; Rolland, C.; Gustafson, L.; Xiao, T.; Whitehead, S.; Berg, A. C.; Lo, W.-Y.; Dollár, P.; and Girshick, R. 2023. Segment Anything. *arXiv:2304.02643*.

Knapitsch, A.; Park, J.; Zhou, Q.-Y.; and Koltun, V. 2017. Tanks and temples: benchmarking large-scale scene reconstruction. *ACM Trans. Graph.*, 36(4).

Lee, J. C.; Rho, D.; Sun, X.; Ko, J. H.; and Park, E. 2023. Compact 3D Gaussian Representation for Radiance Field. *arXiv preprint arXiv:2311.13681*.

Liu, K.; Zhan, F.; Chen, Y.; Zhang, J.; Yu, Y.; Saddik, A. E.; Lu, S.; and Xing, E. 2023. StyleRF: Zero-shot 3D Style Transfer of Neural Radiance Fields.

Liu, K.; Zhan, F.; Xu, M.; Theobalt, C.; Shao, L.; and Lu, S. 2024. StyleGaussian: Instant 3D Style Transfer with Gaussian Splatting. *arXiv preprint arXiv:2403.07807*.

Luan, F.; Paris, S.; Shechtman, E.; and Bala, K. 2017. Deep photo style transfer. In *Proceedings of the IEEE conference on computer vision and pattern recognition*, 4990–4998.

Miao, X.; Bai, Y.; Duan, H.; Wan, F.; Huang, Y.; Long, Y.; and Zheng, Y. 2024. ConRF: Zero-shot Stylization of 3D Scenes with Conditioned Radiation Fields. *arXiv:2402.01950*.

- Michel, O.; Bar-On, R.; Liu, R.; Benaim, S.; and Hanocka, R. 2022. Text2mesh: Text-driven neural stylization for meshes. In *Proceedings of the IEEE/CVF Conference on Computer Vision and Pattern Recognition*, 13492–13502.
- Mildenhall, B.; Srinivasan, P. P.; Ortiz-Cayon, R.; Kalantari, N. K.; Ramamoorthi, R.; Ng, R.; and Kar, A. 2019. Local light field fusion: Practical view synthesis with prescriptive sampling guidelines. *ACM Transactions on Graphics (TOG)*, 38(4): 1–14.
- Mildenhall, B.; Srinivasan, P. P.; Tancik, M.; Barron, J. T.; Ramamoorthi, R.; and Ng, R. 2020. NeRF: Representing Scenes as Neural Radiance Fields for View Synthesis. In *European Conference on Computer Vision*, 405–421. Springer.
- Mu, F.; Wang, J.; Wu, Y.; and Li, Y. 2022. 3d photo stylization: Learning to generate stylized novel views from a single image. In *Proceedings of the IEEE/CVF Conference on Computer Vision and Pattern Recognition*, 16273–16282.
- Müller, T.; Evans, A.; Schied, C.; and Keller, A. 2022. Instant neural graphics primitives with a multiresolution hash encoding. *ACM Transactions on Graphics (ToG)*, 41(4): 1–15.
- Nguyen-Phuoc, T.; Liu, F.; and Xiao, L. 2022. SNeRF: Stylized Neural Implicit Representations for 3D scenes. In *ACM Transactions on Graphics*.
- Oquab, M.; Darcet, T.; Moutakanni, T.; Vo, H. V.; Szafraniec, M.; Khalidov, V.; Fernandez, P.; Haziza, D.; Massa, F.; El-Nouby, A.; Howes, R.; Huang, P.-Y.; Xu, H.; Sharma, V.; Li, S.-W.; Galuba, W.; Rabbat, M.; Assran, M.; Ballas, N.; Synnaeve, G.; Misra, I.; Jegou, H.; Mairal, J.; Labatut, P.; Joulin, A.; and Bojanowski, P. 2023. DINOv2: Learning Robust Visual Features without Supervision.
- Pang, H.-W.; Hua, B.-S.; and Yeung, S.-K. 2023. Locally stylized neural radiance fields. In *2023 IEEE/CVF International Conference on Computer Vision (ICCV)*, 307–316. IEEE Computer Society.
- Reiser, C.; Peng, S.; Liao, Y.; and Geiger, A. 2021. Kilonerf: Speeding up neural radiance fields with thousands of tiny mlps. In *Proceedings of the IEEE/CVF International Conference on Computer Vision*, 14335–14345.
- Simonyan, K.; and Zisserman, A. 2015a. Very deep convolutional networks for large-scale image recognition. In *3rd International Conference on Learning Representations (ICLR 2015)*. Computational and Biological Learning Society.
- Simonyan, K.; and Zisserman, A. 2015b. Very deep convolutional networks for large-scale image recognition. In *3rd International Conference on Learning Representations (ICLR 2015)*. Computational and Biological Learning Society.
- Straub, J.; Whelan, T.; Ma, L.; Chen, Y.; Wijmans, E.; Green, S.; Engel, J. J.; Mur-Artal, R.; Ren, C.; Verma, S.; et al. 2019. The Replica dataset: A digital replica of indoor spaces. *arXiv preprint arXiv:1906.05797*.
- Sun, C.; Sun, M.; and Chen, H. 2022. Direct Voxel Grid Optimization: Super-fast Convergence for Radiance Fields Reconstruction. In *CVPR*.
- Wang, C.; Jiang, R.; Chai, M.; He, M.; Chen, D.; and Liao, J. 2023. Nerf-art: Text-driven neural radiance fields stylization. *IEEE Transactions on Visualization and Computer Graphics*.
- Ye, M.; Danelljan, M.; Yu, F.; and Ke, L. 2023. Gaussian grouping: Segment and edit anything in 3d scenes. *arXiv preprint arXiv:2312.00732*.
- Zhang, K.; Kolkin, N.; Bi, S.; Luan, F.; Xu, Z.; Shechtman, E.; and Snavely, N. 2022. Arf: Artistic radiance fields. In *European Conference on Computer Vision*, 717–733. Springer.
- Zhang, Y.; He, Z.; Xing, J.; Yao, X.; and Jia, J. 2023. Ref-NPR: Reference-Based Non-Photorealistic Radiance Fields for Controllable Scene Stylization. In *Proceedings of the IEEE/CVF Conference on Computer Vision and Pattern Recognition (CVPR)*, 4242–4251.
- Zhou, S.; Chang, H.; Jiang, S.; Fan, Z.; Zhu, Z.; Xu, D.; Chari, P.; You, S.; Wang, Z.; and Kadambi, A. 2024. Feature 3dgs: Supercharging 3d gaussian splatting to enable distilled feature fields. In *Proceedings of the IEEE/CVF Conference on Computer Vision and Pattern Recognition*, 21676–21685.

Reproducibility Checklist

This paper:

- Includes a conceptual outline and/or pseudocode description of AI methods introduced (yes/partial/no/NA): **no**.
- Clearly delineates statements that are opinions, hypothesis, and speculation from objective facts and results (yes/no): **yes**.
- Provides well marked pedagogical references for less-familiar readers to gain background necessary to replicate the paper (yes/no): **yes**.

Does this paper make theoretical contributions? (yes/no) **no**.
If yes, please complete the list below.

Does this paper rely on one or more datasets? (yes/no) **yes**.

- A motivation is given for why the experiments are conducted on the selected datasets (yes/partial/no/NA) **no**.
- All novel datasets introduced in this paper are included in a data appendix. (yes/partial/no/NA) **yes**.
- All novel datasets introduced in this paper will be made publicly available upon publication of the paper with a license that allows free usage for research purposes. (yes/partial/no/NA) **yes**.
- All datasets drawn from the existing literature (potentially including authors' own previously published work) are accompanied by appropriate citations. (yes/no/NA) **yes**.
- All datasets drawn from the existing literature (potentially including authors' own previously published work) are publicly available. (yes/partial/no/NA) **yes**.

Does this paper include computational experiments? (yes/no) **yes**.

- Any code required for pre-processing data is included in the appendix. (yes/partial/no). **no**.
- All source code required for conducting and analyzing the experiments is included in a code appendix. (yes/partial/no). **no**.
- All source code required for conducting and analyzing the experiments will be made publicly available upon publication of the paper with a license that allows free usage for research purposes. (yes/partial/no) **yes**.
- All source code implementing new methods have comments detailing the implementation, with references to the paper where each step comes from (yes/partial/no) **yes**.
- If an algorithm depends on randomness, then the method used for setting seeds is described in a way sufficient to allow replication of results. (yes/partial/no/NA) **NA**
- This paper specifies the computing infrastructure used for running experiments (hardware and software), including GPU/CPU models; amount of memory; operating system; names and versions of relevant software libraries and frameworks. (yes/partial/no) **no**.

- This paper formally describes evaluation metrics used and explains the motivation for choosing these metrics. (yes/partial/no) **no**.
- This paper states the number of algorithm runs used to compute each reported result. (yes/no) **no**.
- Analysis of experiments goes beyond single-dimensional summaries of performance (e.g., average; median) to include measures of variation, confidence, or other distributional information. (yes/no) **no**.
- The significance of any improvement or decrease in performance is judged using appropriate statistical tests (e.g., Wilcoxon signed-rank). (yes/partial/no) **yes**.
- This paper lists all final (hyper-)parameters used for each model/algorithm in the paper's experiments. (yes/partial/no/NA) **yes**.
- This paper states the number and range of values tried per (hyper-) parameter during development of the paper, along with the criterion used for selecting the final parameter setting. (yes/partial/no/NA) **NA**

Methods, Datasets and Experimental Details

Methods

We compare with four SOTA methods:

- **codebase:** We are conducting experiments on lsnerf(Pang, Hua, and Yeung 2023) using its official implementation, and on arf(Zhang et al. 2022), ref-npr(Zhang et al. 2023), and snerf(Nguyen-Phuoc, Liu, and Xiao 2022) using the official implementation of ref-npr(Zhang et al. 2023), which includes the implementations of these three methods.
- **lsnerf**(Pang, Hua, and Yeung 2023): lsnerf is a nerf-based method. lsnerf first trains a segmentation network for 3D scene and use SAM(Kirillov et al. 2023) to generate segmentation mask for style image, and then generate a regions correspondence between 3D scene and style image. Thus lsnerf can perform local style transfer. Three drawbacks for this methods:
 1. Their semantic segmentation only uses cross-entropy loss, so it requires accurate ground truth masks. When the ground truth is not that precise, correct segmentation cannot be achieved.
 2. In general, different regions of the style image are of the same style (the same material and the same texture), but with different colors. Therefore, in most cases, the results generated by lsnerf can only exhibit color diversity and cannot exhibit diversity in texture and material.
 3. Technical problems: we conduct experiments with lsnerf official codebase. It can only work on lff(Mildenhall et al. 2019) datasets. We try replica(Straub et al. 2019) and tnt(Knapitsch et al. 2017) datasets and it doesn't work.
- **snerf**(Nguyen-Phuoc, Liu, and Xiao 2022): snerf proposes a novel training scheme to reduce GPU usage and several loss to transfer style. However,

1. **snr** is capable of learning to transfer the color from a style image, as it relies on statistical methods of image analysis to calculate the loss, which may limit its ability to capture more complex stylistic elements(texture) beyond color.
 2. **snr** refines the geometry but lacks of efficient supervision. In some cases, blurring may occur due to geometric errors.
- **arf**(Zhang et al. 2022): arf proposes nnfm loss to perform precise texture transfer, and deferred back-propagation for memory reduction. However,
 1. nnfm loss uses the VGG(Simonyan and Zisserman 2015a) features of the style and rendering for matching. The VGG features of the same object in different view may match different style feature due to the VGG feature lacks of 3D awareness, lead to the same object displaying different styles from different views.
 2. When rendering the full-resolution image, the deferred back-propagation method still consumes a significant amount of GPU memory.
 - **ref-npr**(Zhang et al. 2023): ref-npr first styles a reference view, then transfer the style of reference view to other views. We use SANET(?) to style reference view with style image. ref-npr introduces the Template-Based Semantic Correspondence (TCM) mechanism, leveraging VGG features for nearest neighbor searches, facilitating the seamless diffusion of stylistic elements from the reference view to alternative perspectives. However,
 1. VGG features have no 3D awareness and using VGG for nearest search across different view can lead to multi-view inconsistency issues.
 2. If the styled reference image contain complex texture details, pixels from certain perspectives may not match to the pixels in the reference view, hence style transfer cannot be performed, resulting in white noise spots.

Discussion of Controllable Style Methods There are some controllable style transfer methods: StyleRF(Liu et al. 2023), ConRF(Miao et al. 2024), ref-npr(Zhang et al. 2023), lsnerf(Pang, Hua, and Yeung 2023). StyleRF require segmentation mask for all training images. For large scenes containing hundreds of images, it is impractical to generate masks for all images, and multi-view consistency cannot be guaranteed; ConRF use Clip(?) to generate segmentation mask for each training image and multi-view consistency cannot be guaranteed; lsnerf trains a segmentation network, but they can only perform segmentation in relatively simple scenes and require accuracy ground-truth masks; ref-npr can control the style of the scene by adjusting the style of the reference view.

StyleRF and ConRF are zero-shot style transfer methods, and ConRF can not handle 360 degree scene(tnt(Knapitsch et al. 2017)) datasets. Thus we did not compare with StyleRF and ConRF.

Datasets

We conduct experiments on two datasets: lfff(Mildenhall et al. 2019) datasets and tnt(Knapitsch et al. 2017) datasets.

- **lfff**(Mildenhall et al. 2019): simple dataset only contains mimic variation of view angles. lfff dataset is too easy for Gaussian Splatting(Kerbl et al. 2023), thus we conduct experiments on more complex 3D scenes(Knapitsch et al. 2017).
- **tnt**(Knapitsch et al. 2017): 360° captures outdoor scenes.

Experiments Explanation

Experiments Explanation for Figure. 4, 8, 6, 7 in regular paper.

- Figure. 4: single style transfer on lfff datasets with two style images shown on Figure. 11.

lsnerf failed to stylize in *flower* scene because the matching mechanism matched different regions in the *flower* scene to a small regions of the style image, which led to the failure in capturing the local style of the style image. In *fern* scene, the images generated by LSNeRF exhibit a monotonous color palette and instances of blurriness, such as in the rendering of leaves.

The primary issues with snr arise from geometric error that lead to multi-view inconsistencies and image blurriness.

arf can generate the desired results in *Style1*. In *Style2*, arf blended all the colors together to render a stylized image with darker hues, resulting in a color mismatch issue.

ref-npr can produce appropriate stylization in *Style1*, but when faced with a more complex stylization image like *Style2*, it tends to generate images that are blurry and unclear. Because relying solely on VGG cannot ensure the consistency of matches across different views. This issue becomes more severe in the *train* scene in tnt(Knapitsch et al. 2017) datasets in Figure. 16.

As shown in Figure. 13, our method can generate more stable results. First, the colors present in the style image can almost all be found in the images our method generate. In contrast, in the *fern* scene on *Style2*, the images generated by ARF lack green color. Second, our method can generate more texture details. Third, our method can perform multi-style transfer.

- Figure. 8: multiple styles transfer on lfff datasets. lsnerf can only perform local style transfer on a single image, whereas ref-npr can perform multi-style transfer on the reference view and then proceed with 3D style transfer. ref-npr may exhibit blurriness at the boundary of different styles because it does not use semantics to accurately segment different objects.
- Figure. 6 and Figure. 7: style transfer on tnt datasets. Compare with these methods,

firstly, our method can generate complete style transfer(Figure 6, the fourth row, ref-npr has overlooked the background);

Secondly, our method can achieve correct color transfer(Figure 6, the third row, *horse* scene, arf generates colors are too dark and do not match the colors of the style image.)



Figure 9: Ablation study of texture. Second row is multi-style loss with local-global matching, first row is nnfm loss(Zhang et al. 2022) with VGG feature matching.

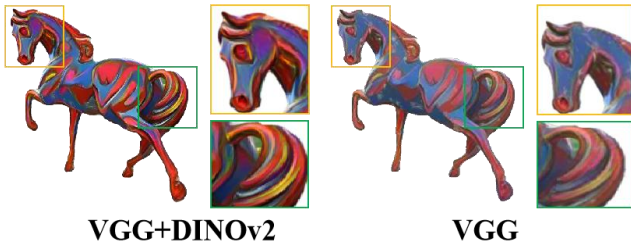


Figure 10: Ablation Study of texture. Left image is multi-style loss with local-global matching, right image is nnfm loss(Zhang et al. 2022) with VGG feature matching.



Figure 11: Figure 4 style images

Thirdly, our method can generate more precise texture. And in multiple styles in Figure 7, our model can ensure that the styles between two different objects do not interfere with each other(Figure 7, the second row, orange box, The styles generated by ref-npr of the foreground and background are mixed together, with the background presents red color).

Additional Experiments

We primarily conducted ablation studies on the style loss and three regularization terms.

Ablation Study

Multi-Style Loss Three advances for multi-style loss: (1) perform multi-style transfer; (2) reduce GPU memory usage; (3) richer texture; (4) multi-view consistency.

- **Multi-Style Transfer:** We segment the scene into multiple parts, each part styles transfer with a different style. As shown in Figure. 12, our multi-style loss can perform multiple style, single and stylization of a single object.
- **GPU Memory Usage:** Because we have divided the scene into different parts, we can optimize a selection of Gaussian points for each part, reducing memory usage. Table. 4 shows the number of Gaussian points that optimized in each iteration.
- **Richer Texture:** Figure. 10 and Figure. 9 demonstrates the effectiveness of our method, capable of learning clearer and richer textural details.
- **Multi-view Consistency:**

As shown in Figure. 14 and Figure. 15, in terms of visual quality, our method can ensure multi-view consistency across different views.

Additionally, we have provided a consistency Table. 3 for all methods. (1) We use the metrics from (Chiang et al. 2022a) to measure the consistency. (2) For a fair comparison, all methods are only stylized in a single style. (3) And we randomly sampled 15 images from both the testing trajectory and the training trajectory, making a total of 30 images for consistency evaluation. ref-npr exhibits poor consistency on the *train* scene, which is why we did not test it on the *train* scene. Our method can achieve the best consistency score in all metrics.

Regularizations Given that the labels for our semantic segmentation are derived from video segmentation(?), which do not guarantee high-quality annotations, we have introduced three regularization techniques to significantly improve the accuracy of our semantic segmentation. KNN smooth regularization ensures the correction of some detail errors, while negative entropy and semantic importance filter ensures the correction of large-area errors. **Negative**

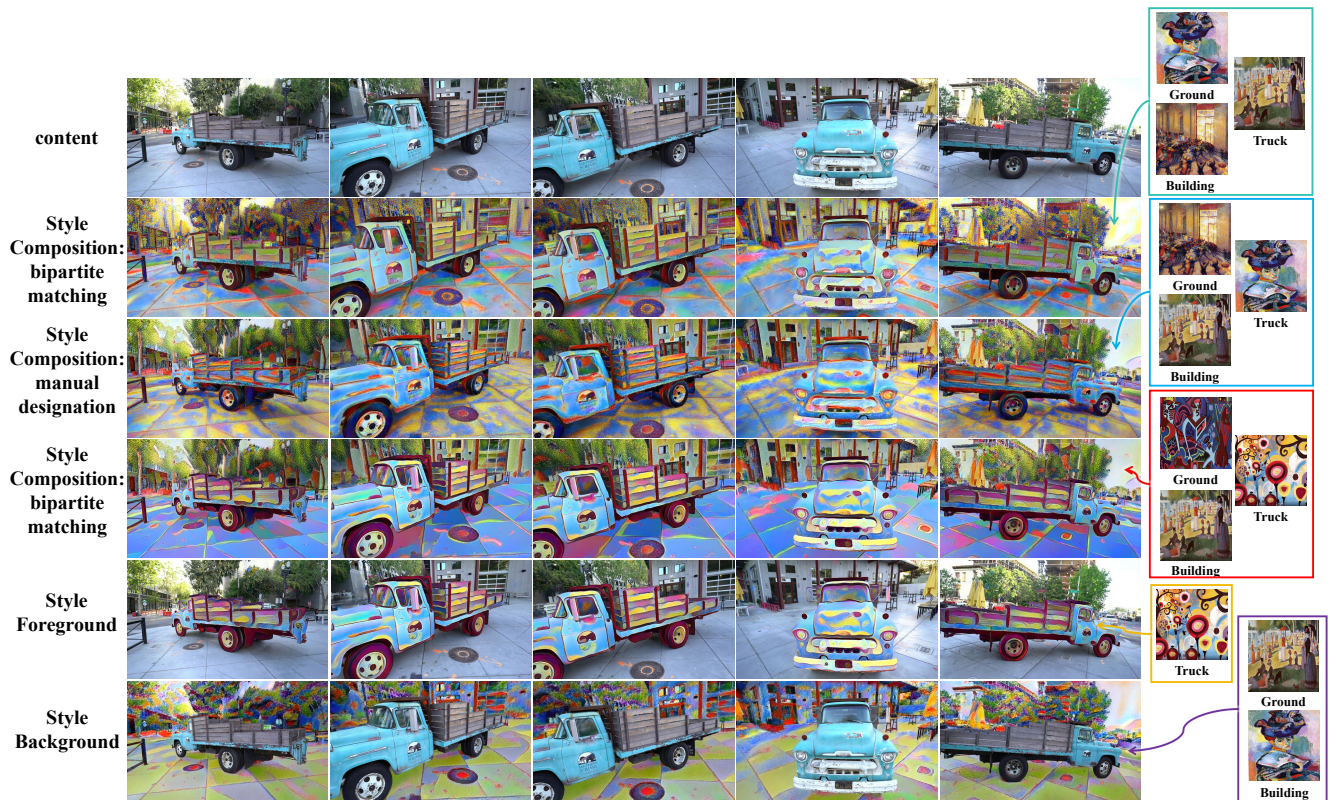


Figure 12: Ablation Study of multi-style transfer of Multi-Style loss. **Second row and third row**: ablation study of the bipartite matching. The style matching can be assigned through an bipartite matching or manual designation; **Second row and fourth row**: ablation study of the diverse style. We can set arbitrary styles for different areas. **Last two row**: ablation study of on a single object. We can specify any object for arbitrary styling.

Methods	truck	horse	Family	flower	Avg.
snerf	3.00	2.7	2.9	0.78	2.35
arf	2.23	1.50	1.43	0.16	1.33
ref-npr	3.12	1.78	1.83	0.88	1.90
ours (vgg)	1.71	1.70	1.53	0.14	1.27
ours	1.55	1.21	1.35	0.14	1.06

Table 3: Quantitative comparisons of multi-view consistency. Lower scores indicate better consistency.

entropy must be used in conjunction with semantic importance filter; Negative entropy identifies Gaussians in the scene with significant semantic content, while semantic importance filter eliminates the remaining Gaussians that do not convey semantic information. Therefore, using negative entropy alone is ineffective. We conduct two ablation study: (1) knn regularization; (2) negative entropy and semantic importance filter. As shown in Figure. 19, our model can ensure the completeness of both segmentation details and the overall integrity.

Additional Experiments

We conduct additional experiments on *train* and *Family* scene in tnt(Knapitsch et al. 2017) to evaluate efficiency.

style loss	truck	horse	train	Family
multi-style loss(our)	362,548.6	301,322.7	378,561.5	333,453.5
nnfm	1,087,646	834,546	756,747	1,232,545
loss(arf)	1,087,646	834,546	756,747	1,232,545
gram	1,087,646	834,546	756,747	1,232,545
loss(snerf)				

Table 4: Ablation Study of GPU memory. Multi-style loss optimizes fewer points each time, using less GPU memory.

Due to the difficulty of the *train* dataset, ref-npr uses 5 styled reference views for stylization.

Figure. 16 and Figure. 17 show the single style transfer on *train* and *family* scene. snerf has produced blurry results due to incorrect geometry; arf can generate decent results, but there are issues with texture blurring and unclear structure; ref-npr(Zhang et al. 2023) leverages VGG features for pixel-level matching across various viewpoints; however, this approach encounters challenges with multi-view consistency. Our model is capable of generating clear and rich details while ensuring multi-view consistency. Additionally, our method can preserve structure information of the orig-

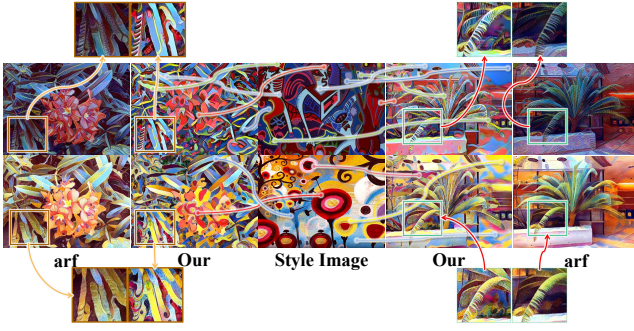


Figure 13: The colors present in the style image can almost all be found in the images we generate. In contrast, the results from arf(Zhang et al. 2022) cannot find the green color in *flower* scene in the first row, and arf generates image with darker hues by blending color. Additionally, our method contain more texture details.



Figure 14: Ablation study of consistency, in the *truck* scene, from various perspectives, the same object may correspond to different VGG features, averaging out the details (as seen in subfigures with orange borders) or displaying varying colors (as seen in subfigures with green borders). DINOv2 enhances the global consistency that VGG features lack, ensuring consistent guidance across different viewpoints.

inal scene(black box in Figure. 0, our method can preserve the texture of the ground).

Figure. 18 shows the multi-style transfer on *train* and *family* scene. ref-npr is unable to transfer the style of the background and cannot distinguish between two different styles, whereas our method can effectively migrate different styles to their respective objects.

Additional Metrics

We present the results of a user study designed to assess visual appeal based on user preferences. We collected scores from 27 participants for each set of stylization results produced by ref-npr, arf, and snerf, and then computed the average scores(scale of ten) for 5 different stylized scenes. In multi-style setting, we randomly combine from 5 different styles. And we conduct user study on *truck*, *horse* and *flower* scenes, in these three scenarios, all comparative methods can generate appropriate stylized results.

As shown in Table. 6, notably, our proposed method outperforms the others, achieving the highest average score.

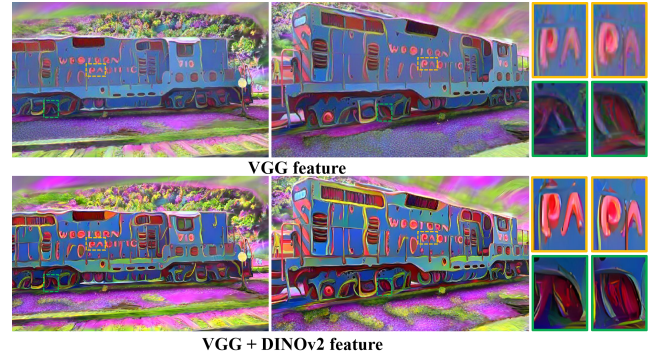


Figure 15: Ablation study of consistency, in the *train* scene, from various perspectives, the same object may correspond to different VGG features, averaging out the details (as seen in subfigures with orange borders) or displaying varying colors (as seen in subfigures with green borders). DINOv2 enhances the global consistency that VGG features lack, ensuring consistent guidance across different viewpoints.

method	styling time
Arf	21.2m
SNerf	184.1m
ref-npr	16.3m
our(vgg)	7.1m
our(single-style)	23.8m
our(multi-style)	22.4m

Table 5: Ablation style of styling time.

Additionally, when we show our multi-style results, most users have raised their scores.

We provide a table showing the average styling time for four methods, as shown in Table. 5.



Figure 16: Additional experiments results on *train* scene in single style setting. **Blue and purple box**: clearer geometry structure; **Black and green box**: texture and details.

score	truck	horse	Flower	avg.
snerf	3.4	3.3	4.0	3.56
arf	7.2	8.0	5.6	6.93
ref-npr	5.2	4.4	7.6	5.73
our(single)	8.2	7.1	7.2	7.50
our(all)	8.6	7.4	7.3	7.76

Table 6: User Study. **our(single)**: we only show the single style transfer results; **our(all)**: we show the single and multiple style transfer results. Most users approve of our multi-style stylization, and our scores have improved after demonstrating the multi-stylized results.



Figure 17: Additional experiments results on *Family* scene in single style setting.

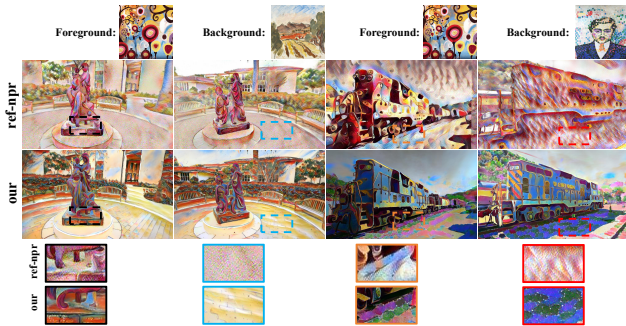


Figure 18: Additional experiments results on *train* and *Family* scene in multiple style setting.

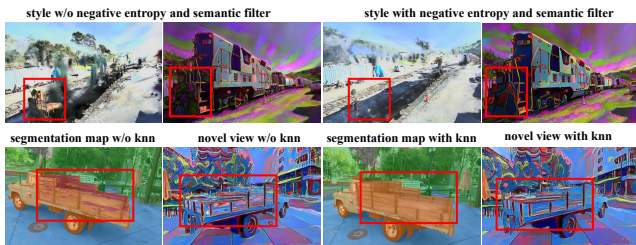


Figure 19: Ablation study of regularization. Our regularization can correctly guide the style, leading to an appropriate stylization.